AECL EACL

AECL CANDU EACL CANDU

Assessing the Mechanical Perfomance of a Fuel Bundle: BEAM Code Description

Third International Conference on CANDU Fuel

1992 October 4-8
Pembroke, Canada

by M. Tayal [i], B.J. Wong [i], J.H.K. Lau [ii], and A.M. Nicholson [iii]

i. AECL CANDU
ii. Ontario Hydro
iii. GEC

92XXXX

AECL CANDU
2251 Speakman Drive
Mississauga Ontario
Canada L5K 1B2

EACL CANDU
2251, rue Speakman
Mississauga (Ontario)
Canada L5K 1B2

ASSESSING THE MECHANICAL PERFORMANCE OF A FUEL BUNDLE: BEAM CODE DESCRIPTION*

M. TAYAL, B.J. WONG, J.H.K. LAU**, A.M. NICHOLSON***

AECL CANDU, Mississauga, Ontario, Canada

ABSTRACT

The computer code BEAM helps assess the mechanical integrity of a fuel bundle. This paper describes the features and the validation of the code.

The focus of the code is to provide a fast and simple tool for calculating the following parameters of a fuel element and of the adjacent endplate: Axial and lateral stiffnesses of the fuel element; spring constants of the endplate; stresses in the endplate and in the endcap/endplate weld; frequency of lateral vibrations (radial and tangential); collapse pressure;and buckling load. On-power effects such as pellet expansion, hourglassing, densification, creep, and fission product swelling, are especially important in these calculations.

The calculations of the code show reasonable agreement with axial and flexural rigidities measured in out-reactor tests using many combinations of sheath and pellet dimensions and using various degrees of pellet/sheath interferences. In addition, the calculations also compare well with measurements of lateral frequencies in out-reactor and in-reactor tests.

The BEAM code is fast: To simulate a typical irradiation history representing a residence period of about 1 year (136 time-steps), the code requires only 12 CP seconds on our CYBER-990 computer. The turnaround time is about 20 seconds.

The BEAM code was used in an investigation of endplate cracking in the Darlington reactor. The calculations suggested that the axial stiffness of the fuel elements is influenced significantly by element power, by pellet densification, and by sheath creep. Another application of BEAM involved the assessment of endplate integrity due to differential axial expansion of fuel elements in a Low Void Reactivity Bundle.

---

* Presented at the Third International Conference on CANDU Fuel, CNS, Pembroke, Canada, 1992 October 4 - 8

** Ontario Hydro, Toronto, Ontario, Canada

*** General Electric Canada (Retired), Peterborough, Ontario

INTRODUCTION

Recent experience [1] with Darlington endplates reconfirms that an important aspect of fuel bundle design is to assess the mechanical integrity of the endplate for in-service loads. The BEAM code assists in that direction. The objective is to provide a fast and simple tool for first-cut calculations of some key parameters related to bundle integrity. The initial results are then followed-up by more detailed assessments of selected parameters.

Towards this end, the BEAM code calculates the following parameters of a fuel bundle: Axial and lateral stiffnesses of the fuel elements; spring constants of the endplate; nominal elastic stresses in the endplate and in the endcap/endplate weld due to lateral vibrations; frequency of lateral vibrations (radial and tangential); collapse pressure; and buckling load.

The code considers the influences of sheaths, pellets, and endplates. The effects of the other fuel elements in the bundle, and of the neighbouring fuel bundle, are also considered.

The approach in BEAM is semi-empirical while the constituent sub-models are physically based. Analytical solutions are used where practical.

The code is still evolving. The purpose of this paper is to describe the current status of the code. We first summarize the features of the code, the models that represent them, and their validation. This is followed by two illustrative examples of past uses of the code for Darlington and for High-Burnup/Low Void Reactivity Fuels. Due to space limitations, the discussions are focused on those aspects of BEAM that are most related to these two applications. Other details will be provided at a later date.

Figure 1 defines the terms used in this paper.

BACKGROUND

Previous investigations [1] have identified that the structural integrity of the endplate can be threatened by excessive cyclic and static stresses. One would also expect this from first principles.

The important sources of endplate stresses are: hydraulic drag; differential axial expansions of fuel elements; pressure pulses; and flow-induced lateral vibrations of fuel elements. These are discussed in turn.

One source of static stresses in the endplate is the axial drag load generated by coolant flow. When the fuel string is supported on latches or on side stops, the drag causes bending of the endplate, resulting in stresses in the endplate. The magnitude of the stress is affected by, among others: the drag load; the load shedding (distribution) among successive bundles; the type of support for the fuel string (e.g. latch vs. side-stop vs. shield plug); the dimensions of the endplate; the geometry of the endplate (stress concentration effects); the stiffness

of the fuel elements (level of support/restraint); the endplate temperature; etc.

Another source of static endplate stress is the differential axial elongation of the fuel elements in the various rings of the endplate. These can also bend the endplate.

One source of cyclic stress is the axial vibration of the fuel elements due to pressure pulses in the coolant. If the frequency of the pressure pulses matches the natural frequency of the fuel string, the string will resonate [1]. This creates alternating bending stresses in the endplate. Fatigue failures can result if the amplitude of vibrations is excessive. The important factors include those noted above for drag. In addition, the frequency and the mode of the axial vibrations of the string are also important. These in turn are influenced by on-power effects such as: sheath collapse; pellet expansion and hourglassing; diametral and axial pellet/sheath interaction; densification; fission product swelling; creep; stress relaxation; cracking; bowing; etc.

Another source of cyclic stress is the lateral vibration of the fuel elements. This is generally induced by coolant flow. The important processes are similar to those noted above for axial vibrations.

A complete analytical assessment of the above factors requires a combination of several computer codes. BEAM provides some of the components, as noted earlier. The remaining components are provided by other codes, such as ELESTRES [2], H3DMAP [3], and MARC [4].

The next section discusses the specific features covered by the BEAM code.

FEATURES OF BEAM

Endplate and Weld

The endplate calculations are based on the model described in Reference 5. The circular ring of the endplate is represented by a circular beam on elastic foundations. The elastic foundations are provided by the fuel elements which act as torsional and translational springs. Using this idealization, Reference 5 provides analytical equations to describe the stiffness of the endplate and the nominal elastic stresses in the endplate ring and in the endcap/endplate weld. BEAM uses these equations.

Flexural Rigidity of the Fuel Element

The flexural rigidity of the fuel element is calculated by considering a composite beam made of the sheath and the pellets.

The individual pellets are treated as being partially cracked due to thermal stresses. The cracked portion is able to support only the compressive loads [6]. This shifts the neutral axis away from the geometric center. The degree of pellet cracking is assumed to be a

function of average pellet temperature. The local temperature in the pellet also influences the local Young's modulus.

The model for the flexural rigidity of the stack of pellets allows for the effect of interfaces between neighbouring pellets. The effect of axial gap/contact is also considered.

The impact of the pellet stack on element rigidity is considered to depend on the diametral and axial interferences between the stack and the sheath. The diametral interfacial pressure is an input to BEAM, and is provided by the ELESTRES code. Ditto for axial interference. Sheath collapse is also considered in this calculation.

Natural Frequency of Lateral Vibrations

These calculations also consider the fuel element as a composite beam, and include the preceding influences of stack rigidity and of interfacial pressure.

The restraining effect of the endplates is considered by representing the endplates as equivalent torsional springs. The spring constant is determined by the method described earlier and includes the stiffening effect of the neighbouring elements.

Rotational inertia effects, and the effects of axial loads, are also included. These calculations are based on Reference 7.

Sheath Collapse

If the differential pressure (coolant minus gas) becomes sufficiently large, the fuel sheath can collapse on the pellets. These calculations consider the sheath strength as a function of sheath temperature, and are based on Reference 8.

Axial Stiffness of the Fuel Element

These calculations consider the following influences: axial gap between the stack and the endcaps; diametral interfacial pressure between the pellets and the sheath; stick/slip between the pellets and the sheath; friction; axial loads; and element bow.

Links with Other Codes

The major link is to the ELESTRES code. The most important input from ELESTRES is the interfacial pressure. Other inputs also provided by ELESTRES include: element geometry; the on-power sizes of the radial and axial gaps; and the temperature distribution within the fuel element. Via this link, the results of BEAM reflect all the processes included in ELESTRES, like: pellet expansion; hourglassing; densification; fission product swelling; cracking; creep; stress relaxation; etc.

BEAM is also connected to Harvard Graphics [9], so that the results can be plotted semi-automatically.

Data transfer between ELESTRES, BEAM, and Harvard Graphics is done electronically via computer data files. The files are created and preserved by the upstream code and passed to the downstream one. This semi-automatic process makes the data-transfer fast and error-free.

THEORY

Interpellet Interfaces

The influence of pellet/sheath interaction on element flexural rigidity was studied experimentally and theoretically in the mid-sixties. Information is readily available for 14 combinations of fuel element diameters, sheath thicknesses, and diametral and axial interferences between the pellets and the sheath. The key data and results are summarized in Table 1. The diametral interference (case 3) was achieved by press-fitting oversized pellets into sheaths. The resulting diametral interference increased the sheath diameter by about 0.3%, which corresponds to an interfacial pressure of about 16 MPa. The axial compression (cases 10 and 13) was likely applied by removing the endcaps and loading the stack by pistons. The fuel element was then bent laterally. "Rigid UO_2" (cases 11 and 14) refers to slugs about 5-8 cm long. All the tests were done in out-reactor rigs.

Figure 2 shows a sample plot of deflection vs load obtained by Twarog [10]. Figure 3 plots the flexural rigidities.

Twarog's tests showed [10] that the flexural rigidity of a complete fuel element is similar to that of an empty sheath.

The rigid pellets were found to increase the flexural rigidity by a factor of 5-8. This is in close agreement with theoretical calculations of a composite beam consisting of the sheath and a solid full-length rod of UO_2.

Twarog's tests also showed [10] that oversized UO_2 pellets in diametral interference with the sheath increase the bending stiffness of the fuel element by a factor of about 2.3. A similar effect was noted for conditions of axial interference - please see Table 1. This factor (2.3) is significantly lower than the effect of rigid UO_2 noted above. This is attributed to the effect of interpellet interfaces, which allow neighbouring pellets to rotate relative to each other. This means that a stack of pellets does not offer as much resistance to bending as would a solid full-length rod of UO_2.

Another evidence for relative rotation of neighbouring pellets comes from measured post-irradiation profiles of fuel elements. Distinct kinks are sometimes seen in the axial profile of element bow. These would be unlikely if the stack of pellets bent as one solid rod.

The relative rotation of neighbouring pellets can be prevented by a sufficiently large axial compressive force on the pellet stack. Simple calculations show that an axial force of ~ 4.7 kN would be needed on an

individual fuel element to prevent relative rotation of adjacent pellets in a fuel element with a midspan lateral deflection of 1 mm. This is a large force, and it is not clear if this can be reasonably expected in an operating fuel element.

BEAM simulates the separation of interfaces by a model that allows compressive stresses to be transmitted between neighbouring pellets, while the tensile forces are not transmitted. This is very similar to the model for cracked pellets documented earlier [6].

The fraction of stack stiffness so affected depends on the number of interpellet interfaces. The interface effect is low if the pellets are long, i.e. less number of interfaces, and vice-versa.

Based on the flexural rigidities measured in the above tests, we deduce that the impact of the interfaces on flexural rigidity is equivalent to 85% cracking in the pellets.

Pellet Cracking

During irradiation, some parts of the pellet crack due to thermal expansion. Also, some of the cracks can heal during the irradiation [11]. Further, the cracks could have a complex orientation with respect to the three main directions (radial, axial, circumferential). Thus, a complex and dynamic distribution of cracks can occur in the pellet during the irradiation.

The cracks can influence the rigidity of the pellet in three ways. Firstly, the radial components of the cracks increase the diameter of the pellet, which either reduces the radial gap or increases the interfacial pressure. This effect is covered by the ELESTRES calculations.

Secondly, the axial component of the cracks can provide extra axial compliance [12], either via closing of the gap in the crack during compressive loading or via slip of adjacent fragments along an inclined crack surface. This reduces the axial stiffness of the pellets.

Thirdly, the axial component of the crack cannot support a net tensile axial stress. This means that the pellet can bend more easily, decreasing its flexural rigidity.

BEAM represents the net effect of interfaces and cracking by an equation of the following form:

$$J_p = f_c J_c + (1 - f_c) J_u$$

This equation defines the net rigidity of the pellet, J_p, as a summation of the rigidities J_c and J_u of the cracked and of the uncracked parts of the pellet respectively. Here f_c represents the fraction of the pellet volume that is cracked.

The rigidity of the uncracked pellet, J_u, is calculated by using the classical equations from solid mechanics [13]. The equations for the rigidity of cracked pellets, J_c, are given in Reference 6.

In these calculations, BEAM accounts for the parabolic temperature profile across the radius of the pellet. This results in non-uniform Young's Modulus within the pellet. To account for it, BEAM subdivides the pellet cross-section into 100 annuli of equal thicknesses. BEAM then integrates for the flexural rigidity using the local Young's modulus in each annulus as a function of the local temperature.

The equation for the Young's modulus is taken from MATPRO-11 [14], and is shown in Figure 4. Note that sufficient and consistent data exist for temperatures upto 1400°C. It is also interesting to note that UO_2 at 1400°C is stiffer than many common metals at room temperature, viz.: bronze, brass, Zircaloy, and aluminum. Thus, it is reasonable to assume that the central parts of the pellet are capable of carrying loads.

Axial Stiffness/Compliance of the Fuel Element

Compliance refers to the axial shortening of the fuel element under an external compressive axial load. Stiffness is the inverse of compliance and quantifies the axial load required for unit shortening of length. The definitions are as follows:

$$\text{Compliance} = C = dl/dF$$
$$\text{Stiffness} = K = dF/dl$$

Here, dF represents an incremental axial compressive load, and dl represents the resulting incremental compression.

For modelling the compliance of a fuel element, the following five components of deflection can be postulated from first principles: axial compression of the sheath; axial compression of the pellets; bending/bowing of the fuel element; axial compression of the endcap; and axial compression of the endcap/endplate weld.

Sensitivity studies show that the last two effects noted above are insignificant compared to the first three. This is largely because the lengths of the endcap and of the endplate weld are very small compared to the sheath. For this reason, these two components are not discussed any further. The remaining three components are described in the following paragraphs.

Sheath Compression

The axial compression of the sheath refers to the shortening of the length of an individual fuel sheath under a compressive load. The parameters that govern sheath compression are the Young's modulus of the sheath, the cross-section area of the sheath, and length of the sheath. During irradiation, the following processes can affect the axial stiffness of the sheath:

Temperature. The temperature of the sheath is higher on-power than zero power cold. Higher temperature lowers the Young's modulus and tends to reduce the element stiffness.

Collapse. Under in-reactor conditions of elevated temperature and pressure, the sheath can collapse (diametrically) onto the pellets, either instantaneously or slowly via creep. Sheath collapse will result in pellet/sheath contact, which will lead to a stiffer fuel element. The rate and extent (e.g., area and pressure) of collapse will depend on a variety of factors such as: microstructure of the sheath; dimensions of the sheath; diametral clearance; temperature; differential pressure; rate of creep of the sheath; etc.

Elastic Compression. The coolant pressure compresses the sheath and reduces the diametral and axial clearances with the pellet.

Thermal Expansion. Thermal expansion of the sheath increases the clearances.

Creep. Creep of the sheath leads to reduced clearances if the sheath is not in contact with the pellets. If the sheath is already touching the pellets, sheath creep leads to relaxation of interfacial pressure.

Pellet Compression

The pellets can also contribute to the stiffness of the fuel element if there is a tight diametral or axial contact between the pellets and the sheath and/or the endcaps. In unirradiated fuel elements, the pellets and the sheath are separated by axial and diametral clearances, hence, the pellet does not participate in the axial stiffness.

During irradiation, a variety of conditions in the reactor can lead to pellet/endcap and/or pellet/sheath contact. With (axial) pellet/endcap contact, some of the compressive axial load can be transmitted to the pellets via the endcaps. With (diametral) pellet/sheath contact, some axial load can be transmitted to the pellets via friction. Both these situations will result in fuel element stiffening.

The degree of element stiffening caused by the pellet depends on the following factors:

- Diametral interfacial pressure between the pellet and the sheath,
- Axial interference between the endcaps and the pellets, and
- Local stiffnesses of the various radial regions of the pellets.

The above, in turn, are influenced by a number of processes, design features, material properties, and operational parameters. These include:

Diametral Expansion. Due to thermal expansion, the pellet contacts the sheath.

Hourglassing. The diametral expansion of the pellet is not uniform along the length of the pellet. Rather, the ends of the pellet expand more than the middle parts of the pellet, due to end effects. This is called hourglassing. It increases the average interfacial pressure between the sheath and the pellet.

Densification. In-reactor sintering of UO_2 reduces the diameter of the pellet, which lowers the interfacial pressure.

Fission Product Swelling. This increases the diameter of the pellet, increasing the interfacial pressure.

Axial Expansion. Under some conditions, thermal expansion of the pellets can cause axial contact between the endcaps and the pellet stack.

Pellet Cracking. As noted earlier, thermal stresses in the reactor can cause cracking in the brittle parts of the pellet. Some of the cracks can subsequently "heal" due to creep. A cracked pellet is softer than an uncracked one.

Temperature Profile. Again as discussed earlier, the pellet is much hotter in the centre than at the surface. The Young's Modulus is lower in the hotter regions.

Slip. Where there is pellet-to-sheath contact and an axial gap, the degree to which the pellet stiffens the fuel element depends on the extent of axial slip between the sheath and the pellet. The slip in turn depends on: the area of contact; the coefficient of friction; the axial load; and the interfacial pressure (hoop).

Dishes/Chamfers. Dishes/Chamfers and their non-uniform axial thermal expansion create an uneven surface at the end of the pellet. Hence two neighbouring pellets do not contact over their full diameter. The fraction of the pellet diameter that is not in contact does not transfer axial load. Therefore the portion of the pellet near the uncontacted area does not contribute to the axial stiffness of the fuel element. The extent of this effect depends on the on-power profile of the pellet face, which in turn depends on: the initial sizes of the dish and chamfer; element power; thermal expansion; densification; creep; and fission product swelling. Although this is a significant effect, at present it is not included in the BEAM code and needs to be considered separately. The brief discussion above is included here for completeness.

The net effect of the pellet stack on the stiffness of the fuel element is given by a sum of the individual influences noted above.

Element Bending/Bowing

Fuel elements exhibit a certain degree of lateral bending due to:

- As-manufactured bows, and
- Circumferential temperature gradients in the reactor.

An axial force increases the bend which in turn decreases the axial length. This is another source for element compliance. The governing parameters are the flexural rigidity, the length of the element, and the magnitude of bow.

VALIDATION

To check the validity of our understanding and modelling, calculated stiffnesses were compared to the available stiffness measurements for the following situations: Unirradiated fuel elements with and without interference-fitted pellets; Irradiated fuel elements; Fuel element plus pieces of endplates; and Complete fuel bundles. For the latter two conditions, the calculations of BEAM for element stiffness were supplemented with separate calculations for the effects of endplates. In addition, calculated frequencies of lateral vibrations of fuel elements were also compared to available measurements for off-power conditions and for on-power conditions.

Unirradiated and Irradiated Fuel Elements without Pellet Interference

Axial stiffnesses of irradiated and unirradiated fuel elements were measured off-power during 1992. Some tests were done in the Fuel Element Axial Stiffness Testing Rig (FEASTER) at Chalk River Laboratories. Other tests were done in an Instron machine at AECL CANDU. Figure 5 compares the measurements vs calculations of BEAM. A reasonable agreement is indicated.

Unirradiated Fuel Elements with Pellet Interference

As noted earlier (section on Interpellet Interfaces), flexural rigidities of 14 combinations of element diameters, sheath thicknesses, and pellet interferences were measured in mid-sixties. The measured rigidities ranged from 54 to 1214 Nm^2. Of these, two specimens contained features that are not included in the BEAM code, viz. trefoil (specimen #6) and U_3Si pellets (specimen #7). The measured rigidities of the 12 remaining specimens are compared to the calculations of BEAM in Figure 6. A strong agreement is evident.

Fuel Elements with Pieces of Endplates

Two compression tests are available for single fuel elements from a 37-element bundle with pieces of endplates still attached to the test elements.

The first test used the outer ring, and the endplate pieces were not clamped. Figure 7(a) shows the results. In a fuel bundle, symmetry would dictate zero slope at the centre of the endplate segment between the adjacent fuel elements. In this test, however, no attempt was made to maintain this condition. This results in a lower effective stiffness in the test. Our calculations always assume that the symmetry condition noted above exists. This difference needs to be borne in mind when comparing the measurements with the calculations shown in Figure 7(a).

The second test used the intermediate ring, and the ends of the endplate were clamped to achieve the symmetry noted above. The measurements are given in Figure 7(b), along with the corresponding calculations. Note that the outer ring has a smaller width than the intermediate ring, giving a lower stiffness in the latter.

Complete Fuel Bundle

Reference 1 describes some tests on bundle compression. Figure 8 shows a comparison of measured vs calculated stiffnesses. In general, the calculations show a reasonable agreement with the measurements. Further details are available from Reference 1.

Out-Reactor Lateral Frequency

Out-reactor measurements on Darlington fuel bundles showed that the natural frequency of lateral element vibration is about 30 Hz at room temperature. The BEAM code also predicts 30 Hz.

On-Power Lateral Frequency

Element natural frequencies for lateral vibrations were measured on-power in experiment U-118 [15]. An instrumented G-1 fuel bundle was used. The measured frequencies ranged from ~ 40 Hz at zero power, to ~ 60 Hz at high power. The equivalent increase in the flexural rigidity is a factor of about 2.3. This is very similar to the increase reported by Twarog [10] in his bending tests on fuel elements with interference fit.

To simulate the on-power effects, we first used the ELESTRES code to calculate the on-power behaviour of the element. The results were provided as input to the BEAM code to calculate the on-power frequency of the fuel element for two start-up cycles as a function of power and time. Figure 9 shows that the calculations are in reasonable agreement with the measurements.

ILLUSTRATIVE EXAMPLES

The BEAM code has recently been used in two investigations. The first involved an investigation of the failures of Darlington endplates [1]. The second involved design assessments of a fuel bundle being designed for low void reactivity and for very high burnups [16]. Brief descriptions of the above applications are given here.

Cracking of Darlington Endplates

Activities in fuel and fuel string modelling were undertaken as a part of the overall program to determine the cause of fuel damage in Darlington Units 1 and 2 [1]. The aim was to establish the fuel response in a fuel channel under conditions of hydraulic drag load and pressure pulses. The effects of power (e.g. pellet expansion) and of time (e.g. creep, densification, etc.) were included. The BEAM code provided one component of the calculations (element stiffness); the remaining components were provided by other codes such as ELESTRES (pellet response) and H3DMAP (fuel string response). Hand calculations as appropriate were also used (e.g. endplate stiffness and creep).

The work was done by the Fuel and Fuel String Modelling Team which was assembled by the Darlington N12 Investigation Team. Apart from some of the co-authors of this paper, significant contributions were also made by a number of individuals including: E. Nadeau, W. Teper, F. Iglesias, and P. Ried of Ontario Hydro; M. Pettigrew and B. Smith of AECL-CRL; and I.E. Oldaker and R. Mak of AECL-CANDU. A detailed description of the assessments has been published previously [1]. A brief summary is given here.

The assessment showed [1] that irradiation has a large effect on the stiffnesses of the individual fuel elements. Upon initial startup, the element stiffness is predicted to increase rapidly since thermal expansion causes the pellet to interact with the sheath. Element stiffness is reduced upon UO_2 densification, which occurred for the Unit 2 power history at about 1500 hours from startup. About 200 hours later, the stiffness is predicted to increase to the previous value. This is largely due to creep of the sheath under coolant pressure, with some additional contribution from fission product swelling of the pellet. Element stiffness is predicted to decrease if there is a significant power drop, such as in a 35% reactor power reduction, or during fuelling when high power bundles are shifted into the position of lower bundle power. These trends are shown in Figure 10. The natural frequency of the fuel string increases with the stiffness.

Endplate waviness/compliance, representing a softer spring than the fuel element, moderates the increase in the fuel string stiffness from fuel element stiffening. However, endplate compliance will be removed by Zircaloy creep during irradiation. The creep rate is expected to be higher for downstream bundles due to the higher hydraulic load.

The assessment also showed [1] that the fuel string has a large number of axial modes of vibration. The fifth axial mode of the fuel string has a natural frequency close to 150 Hz. This mode is possibly the way in which the fuel strings responded to the 150 Hz pressure pulses in Unit 2, leading to the observed fuel damage.

It is possible that the fuel string natural frequency (Mode 5) would change during Unit 2 power operation, to coincide with the frequency of the dominant pressure pulses (150 Hz) measured in the reactors. This would lead to resonance of the fuel string. However, because of the non-linearity of the fuel bundles, it does not appear that the difference between resonance and off-resonance response is large. Thus, the fuel string response is likely dominated by the acoustic pressure wave in the fuel channel.

Low Void Reactivity Bundle

One evolution of fuel design is aimed at a CANDU fuel bundle with low void reactivity in combination with very high burnups [16]. One aspect of this design involves using dysprosium in the central fuel elements. This increases the gradient of element powers through the diameter of the bundle. This leads to greater bending of the endplate. To assess the impact of bending on endplate integrity, the BEAM code was used in conjunction with codes ELESTRES and MARC. Elastic-plastic calculations were done.

The endplate was represented by about 1500 thick-shell finite elements from the MARC library. Two approaches were considered to account for the restraints provided by the fuel elements to the endplates: (i) using finite elements to also represent the fuel elements, or (ii) using equivalent springs, with spring constants provided by the BEAM code.

In terms of accuracy, both approaches gave similar results as shown in Figure 11. The figure shows endplate ring deflections using the two approaches. The slight difference in absolute displacements is due to small differences in the boundary conditions used for the outer ring. However, the gradients of displacements are similar. Since endplate stresses and strains are determined by the displacement gradients, the predicted stresses/strains are expected to be similar using either method of accounting for the effect of fuel elements.

In terms of cost, using finite elements to model the fuel pencil/endplate restraints increases the computing cost by a factor of about 10 (i.e. ~ 17 CPU hours vs. 1.7 CPU hours) over using the equivalent springs approach. This translates into a computing cost of about $7,500 per run if MARC alone is used, vs. about $750 per run if MARC is used in conjunction with BEAM. Turnaround time is estimated to be overnight for the springs approach versus several days for the all-finite- elements approach. These comparisons demonstrate the advantages of using BEAM as part of endplate analyses.

COMPUTING COST AND TURNAROUND

To simulate a typical irradiation history representing a residence period of about 1 year (136 time-steps), the BEAM code requires about 12 CP seconds on our CYBER-990 computer. This translates into a computing cost of about $2.

CONCLUSIONS

The computer code BEAM helps assess the mechanical integrity of a fuel bundle. The focus of the code is to provide a fast and simple tool for calculating the following parameters of a fuel element and of the adjacent endplate: Axial and lateral stiffnesses of the fuel element; spring constants of the fuel element and of the endplate; stresses in the endplate and in the endcap/endplate weld; frequency of lateral vibrations (radial and tangential); sheath collapse; and buckling load.

In calculating the above parameters, the following features and effects are considered: sheath; pellets; endplates; other fuel elements in the bundle; instantaneous collapse of the sheath; diametral and axial gap/interference between the pellets and the sheath; inter-pellet interfaces; slip/grip between the sheath and the pellets; irradiation-induced cracking of UO_2 pellets; bowing; hydraulic drag; and temperature-dependent material properties. A semi-empirical approach is used while employing mechanistically-based submodels.

One important aspect of the assessments is to account for on-power effects like: pellet expansion; hourglassing; creep; densification; and cracking. To facilitate that, semi-automated links are provided to connect BEAM with some related codes such as ELESTRES and Harvard Graphics.

The calculations of the code show reasonable agreement with flexural rigidities measured in out-reactor tests using many combinations of sheath and pellet dimensions. In addition, the calculations also compare well with measurements of lateral frequencies in out-reactor and in-reactor tests.

The BEAM code is fast: To simulate a typical irradiation history representing a residence period of about 1 year (136 time-steps), the code requires only 12 CP seconds on our CYBER-990 computer.

The BEAM code was used in an investigation of endplate cracking in the Darlington reactor. The calculations suggested that the axial stiffness of the fuel elements is influenced significantly by element power, by pellet densification, and by sheath creep. Another application of BEAM involved the assessment of endplate integrity due to differential axial expansion of fuel elements in a Low Void Reactivity Bundle.

ACKNOWLEDGEMENTS

We acknowledge M. Gabbani (AECL-CANDU) for his contribution to the bundle compression tests, M. Pettigrew (AECL-CRL) for his contribution to the stiffness tests on irradiated fuel, the Fuel and Fuel String Modelling Team for the Darlington assessments, and F. Iglesias (OH) for discussions on pellet cracking and healing.

REFERENCES

(1) J.H.K. LAU, M. TAYAL, E. NADEAU, M.J. PETTIGREW, I.E. OLDAKER, W. TEPER, B. WONG, F. IGLESIAS, "Darlington N12 Investigation: Modelling of Fuel Bundle Movement in Channel Under Pressure Pulsing Conditions", 13th Annual Conference, Canadian Nuclear Society, St. John's, New Brunswick, Canada, June 1992.

(2) M. TAYAL, "Modelling CANDU Fuel under Normal Operating Conditions: ELESTRES Code Description", Atomic Energy of Canada Limited, Report AECL-9331, 1987.

(3) R.J. SAUVE, E. NADEAU, "H3DMAP, A General Three-Dimensional Finite Element Computer Code For Linear and Non-Linear Analysis of Structures: Users' Manual and Verification Cases", Ontario Hydro Research Division Report #89-221-K, Rev. 1, April 1991.

(4) "MARC General Purpose Finite Element Program: Volumes A to D", MARC Analysis Research Corporation, Palo Alto, California, USA, Revision K.3, July 1988.

(5) M. TAYAL, C.K. CHOO, "Fatigue Analysis of CANDU Nuclear Fuel Subjected to Flow-Induced Vibrations", Atomic Energy of Canada Limited, Report AECL-8331, 1984.

(6) M. TAYAL, "Modelling the Bending/Bowing of Composite Beams such as Nuclear Fuel: The BOW Code", Nuclear Engineering and Design, 116 (1989), pp. 149-159.

(7) R.D. BLEVINS, "Formulas for Natural Frequency and Mode Shape", Van Nostrand Reinhold Company, New York, 1979.

(8) G.H. BRYAN, "Application of the Energy Test to the Collapse of a Long Thin Pipe Under External Pressure", Cambridge Phil. Soc. Proc., Vol. 6, 1888.

(9) "User's Manual for Harvard Graphics 3.0", by Software Publishing Corporation, Mountain View, CA, USA, 1991.

(10) W. Twarog, "Fabrication of Interference Fit Fuel and Comparative Rigidity Tests", Canadian General Electric Company Limited, Report FE-23, 1964 September.

(11) A.S. BAIN, "Cracking and Bulk Movement in Irradiated Uranium Oxide Fuel", Atomic Energy of Canada Limited, Report AECL-1827, 1963.

(12) R.W. WILLIFORD, D.D. LANNING, "Cracked Fuel Mechanics", From Water Reactor Fuel Element Performance Computer Modelling, J.H. Gittus, ed., Applied Science Publishers, London, 1983, pp 153-186.

(13) S.P. TIMOSHENKO, J.M. GERE, "Mechanics of Materials", D. Van Nostrang Company, New York, 1972.

(14) D.L. HAGRMAN, G.A. REYMANN, "MATPRO - Version 11: A Handbook of Material Properties for Use in the Analysis of Light Water Reactor Fuel Rod Behaviour", EG & G Idaho Inc., Report NUREG/CR-0497, TREE-1280, R3, 1979.

(15) M.J. PETTIGREW, "Flow-Induced Vibration Analysis of Nuclear Components", Atomic Energy of Canada Limited, Report AECL-6219, 1978 August.

(16) M. GACESA, P.G. BOCZAR, J.H.K. LAU, P.T. TRUANT, N. MACICI, E.G. YOUNG, "Canadian Fuel Development Program", Third International Conference on CANDU Fuel, CNS, Pembroke, Canada, 1992 October 4 - 8.

TABLE 1: FLEXURAL RIGIDITY OF FUEL ELEMENT

Case No.	Element Type	Sheath Outer Diameter (mm)	Sheath Thickness (mm)	Comments	Flexural Rigidity (Nm^2)	
					Previous Data	BEAM
1	Empty Sheath, Pickering Size	15.24	0.46		54	56
2	Standard Pickering Fuel Element	15.24	0.46		54	56
3	Interference-fit Pickering Element	15.24	0.41	Diametral Interference	124	166
4	19-Element Split-Spacer Bundle	15.24	0.41		57	51
5	28-Element Split-Spacer Bundle	15.24	0.41		63	51
6	Trefoil in PHW Bundle	15.24	0.41	Trefoil	185	Note 1
7	U_3Si Fuelled Element, G-1 Size	19.74	0.97	U_3Si pellets	428	Note 2
8	Standard G-1 Fuel Element	19.74	0.58		154	157
9	Empty Sheath, G-1	19.74	0.53		154	144
10	Sheath plus UO_2 in Axial Compression, G-1	19.74	0.53	Axial Interference	416	431
11	Sheath plus Rigid UO_2, G-1	19.74	0.53		1214	1367
12	Empty Sheath, WR-1	15.24	0.64		74	76
13	Sheath plus UO_2 in Axial Compression, WR-1	15.24	0.64	Axial Interference	195	176
14	Sheath plus Rigid UO_2, WR-1	15.24	0.64		402	459

Note 1: Not Calculated: Effect of Trefoil is not simulated in BEAM

Note 2: Not Calculated: Material properties of U_3Si are not included in BEAM.

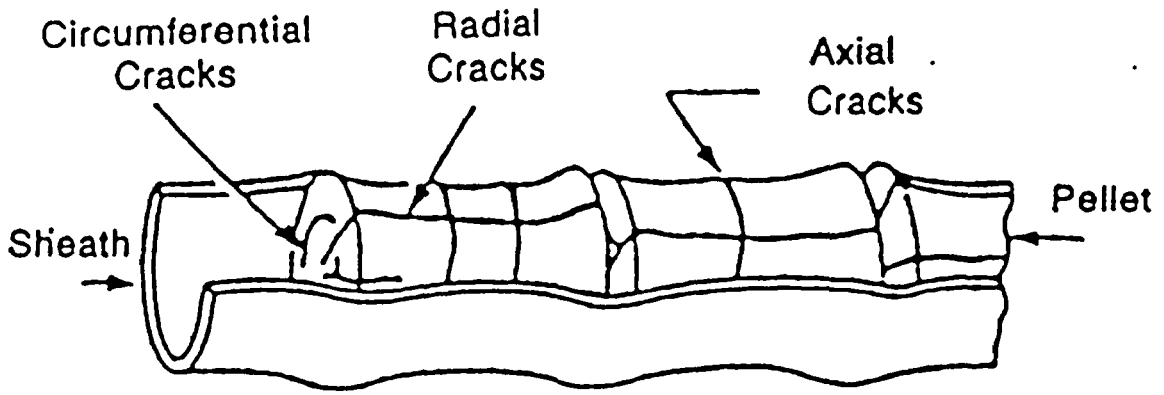

Possible Cracks in a Pellet

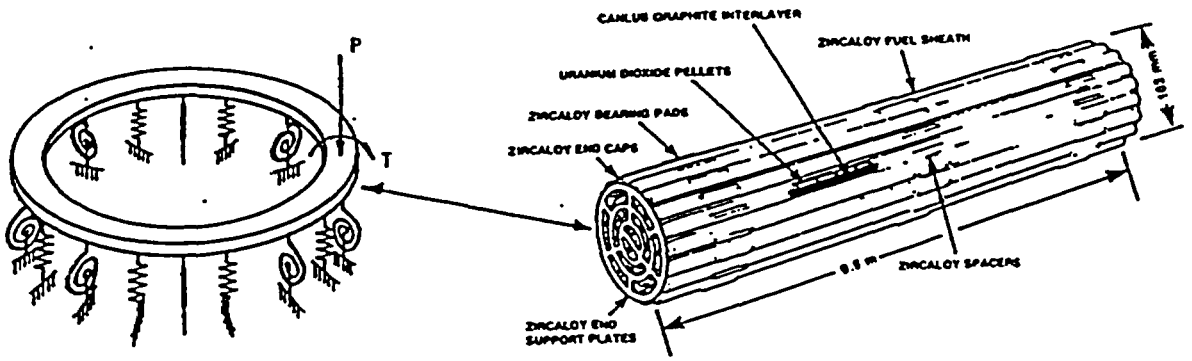

MODEL USED TO REPRESENT AN ENDPLATE AS A CIRCULAR RING ON ELASTIC TRANSLATIONAL AND TORSIONAL FOUNDATIONS.

Fuel Bundle

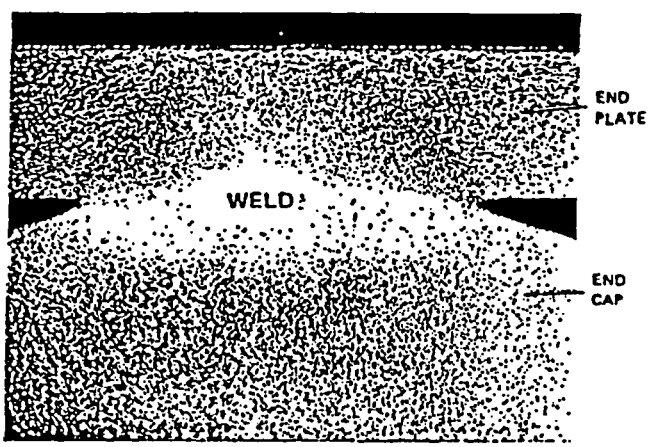

CROSS-SECTION OF BUNDLE ASSEMBLY WELD

R.D. Page, "Canadian Power Reactor Fuel", AECL-5609, 1976 March.

FIGURE 1 DEFINITIONS OF TERMS

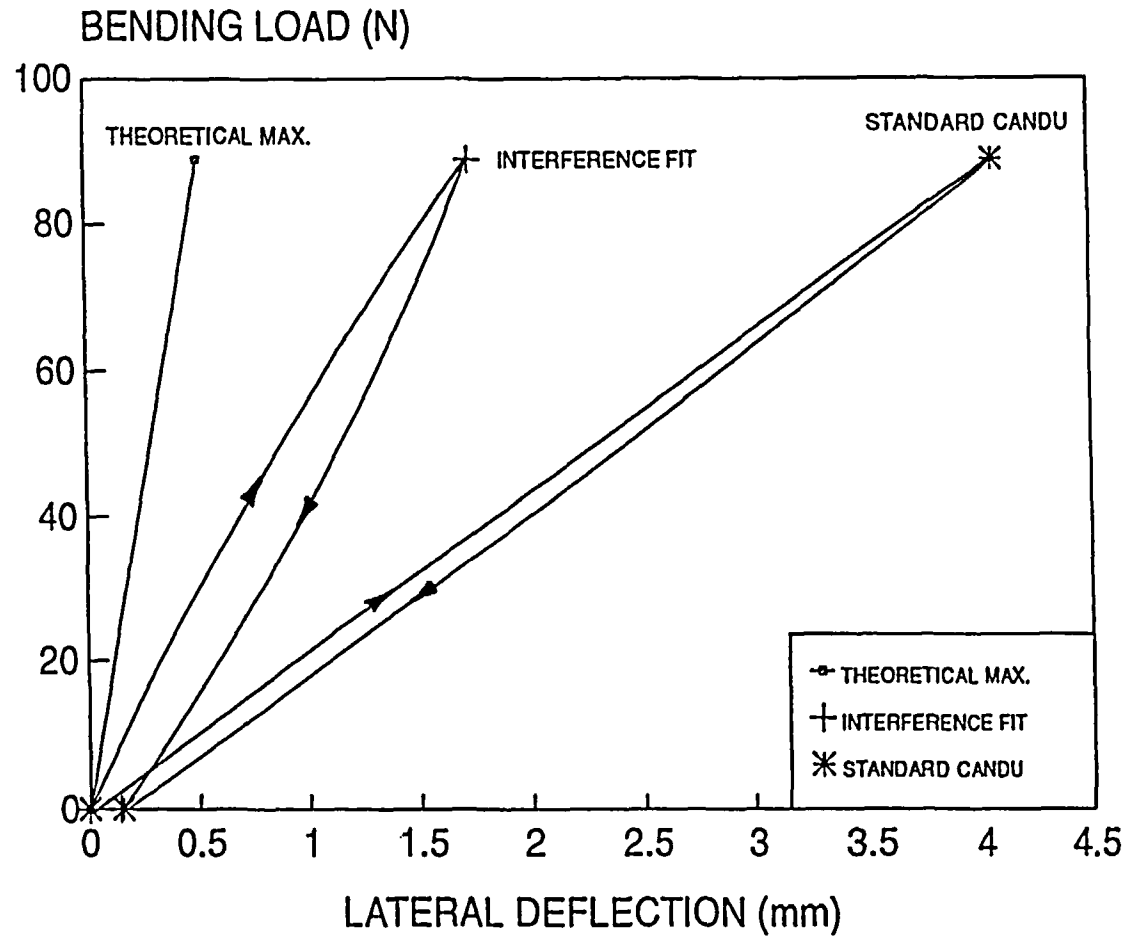

FIGURE 2: IMPACT OF INTERFERENCE FIT ON ELEMENT FLEXURAL RIGIDITY

(THEORETICAL MAX. = SOLID UO2 ROD PLUS SHEATH)

EI RESULTS CORRECTED FOR SHEATH THICKNESS

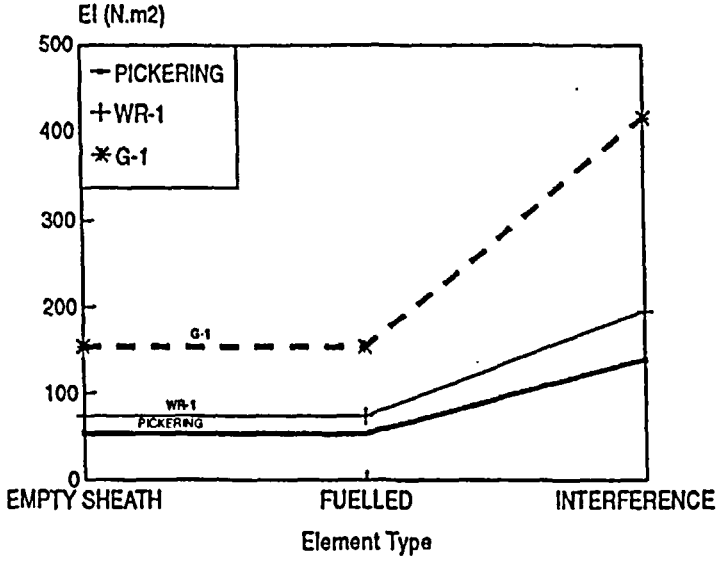

a) Effect of Pellet Interference

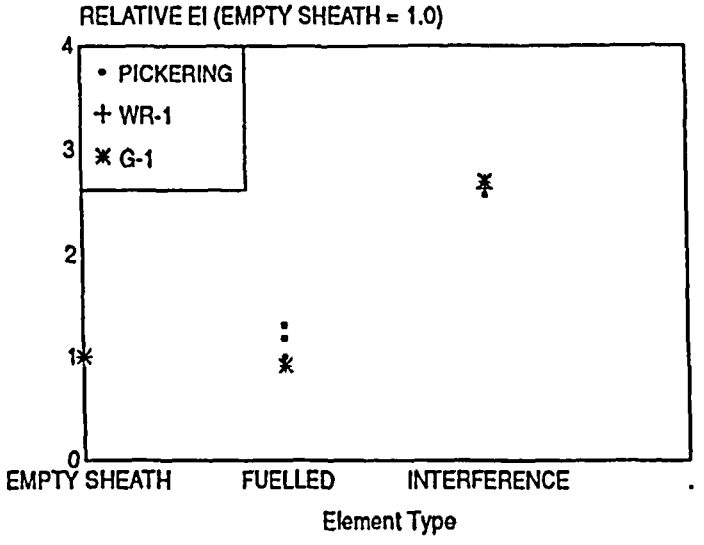

b) Relative Effect of Pellet Interference
(Ratio relative to empty sheath)

FIGURE 3: EFFECT OF PELLET/SHEATH INTERFERENCE ON ELEMENT FLEXURAL RIGIDITY

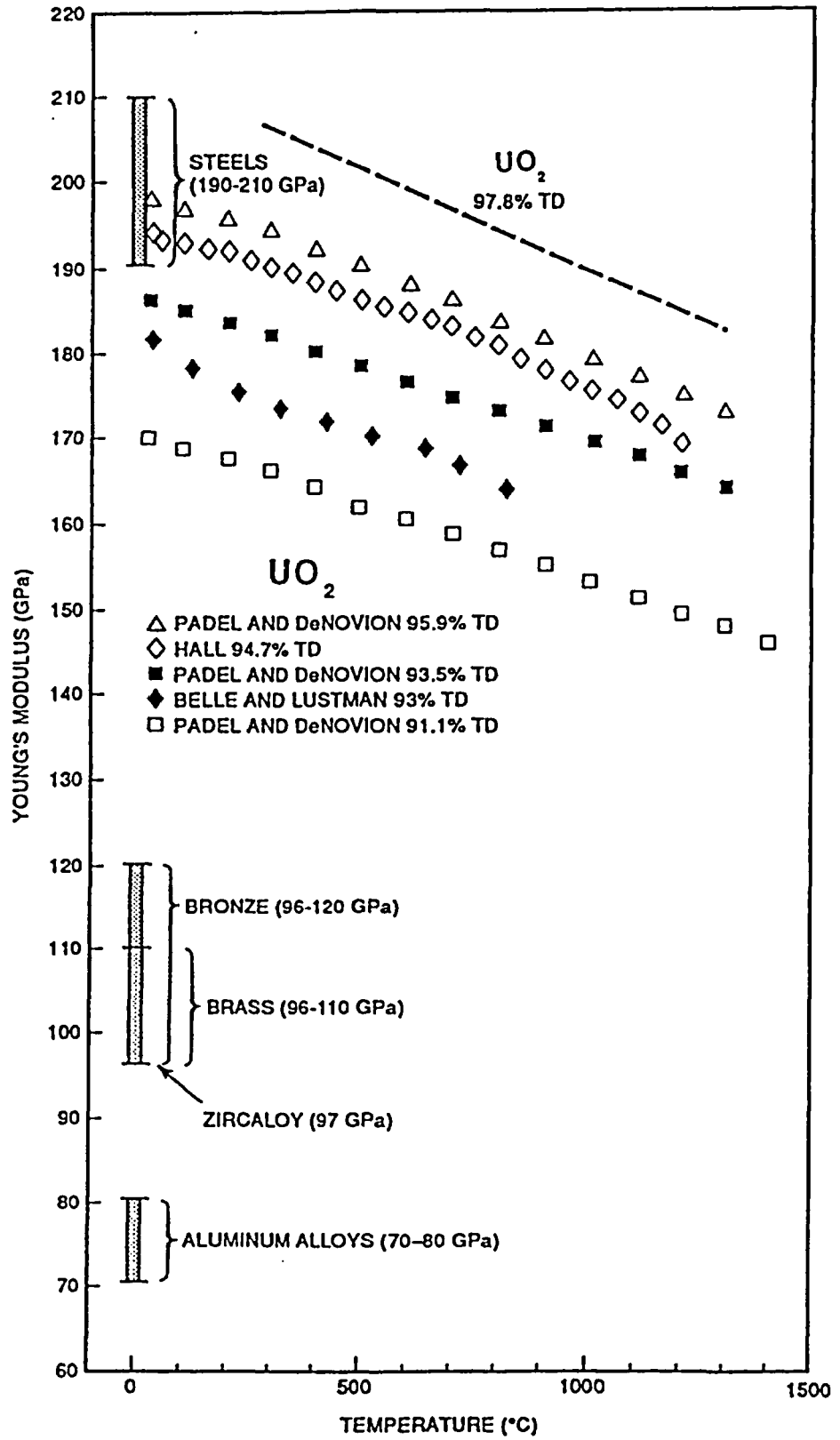

FIGURE 4: YOUNG'S MODULUS OF UO_2
(TD: THEORETICAL DENSITY)

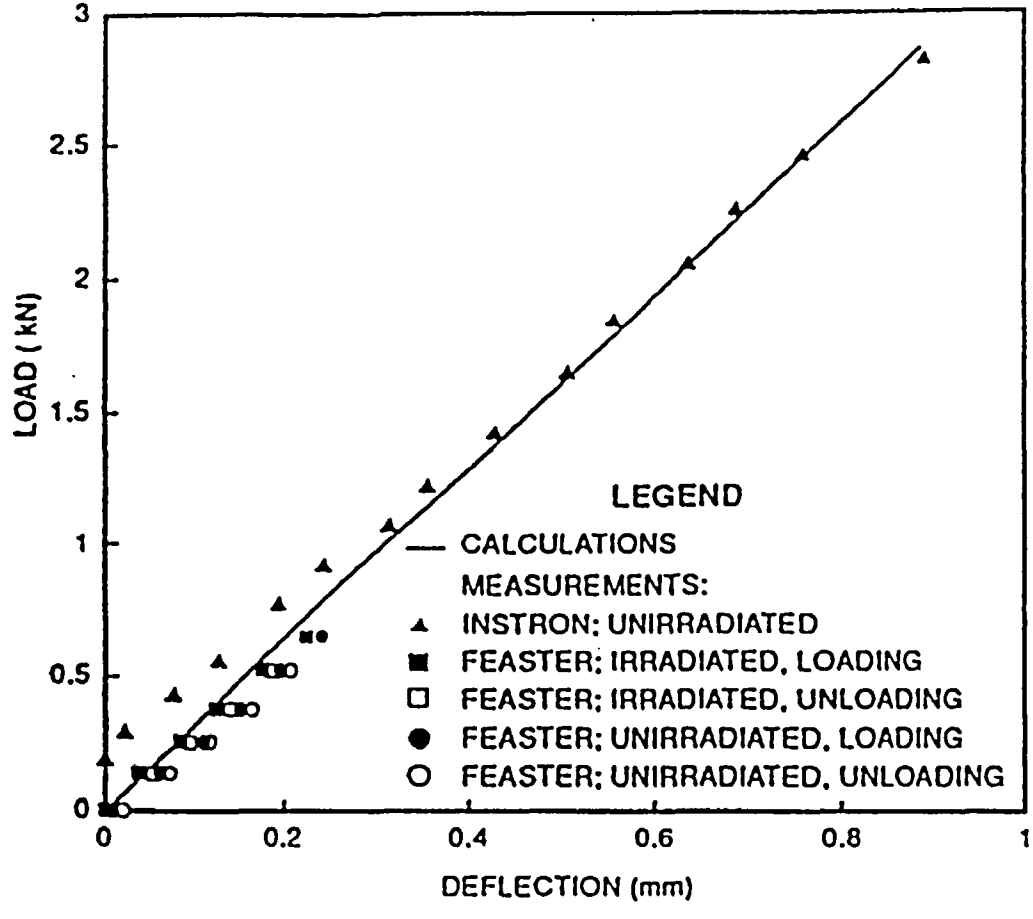

FIGURE 5: SINGLE ELEMENT AXIAL STIFFNESS: CALCULATED(BEAM) vs. MEASURED

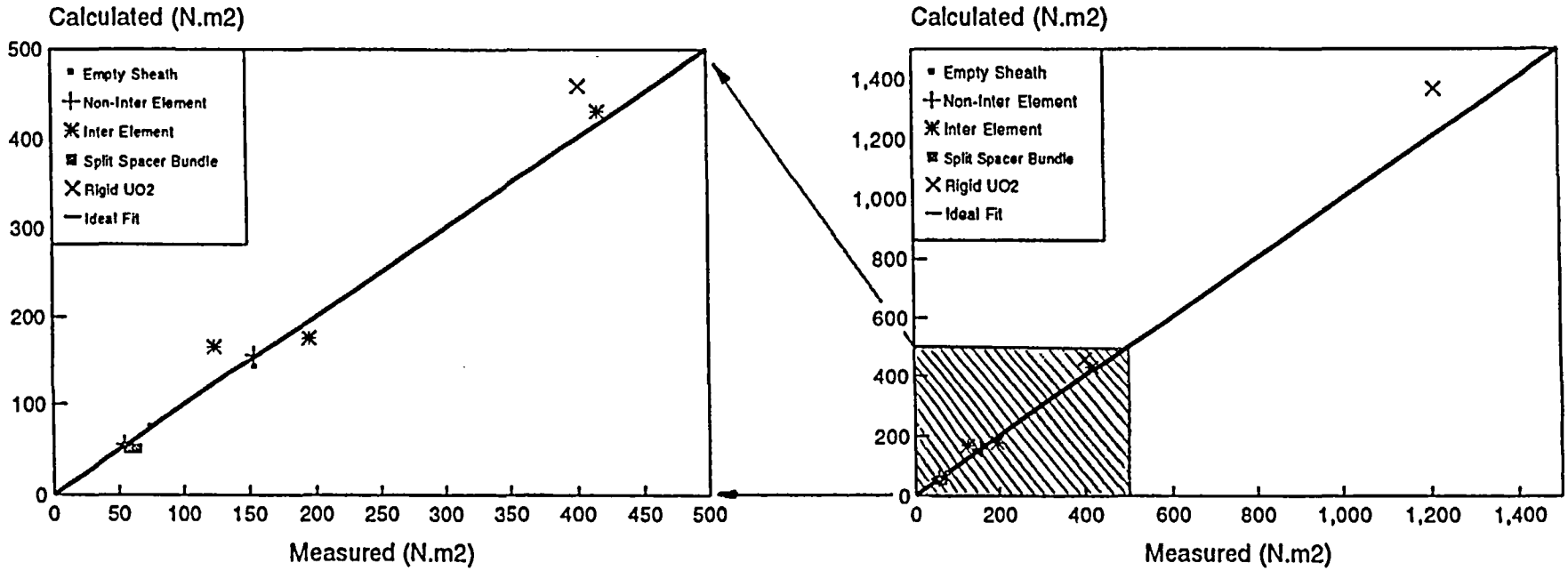

FIGURE 6: VALIDATION OF FLEXURAL RIGIDITY CALCULATIONS INCLUDING PELLET/SHEATH INTERFERENCE

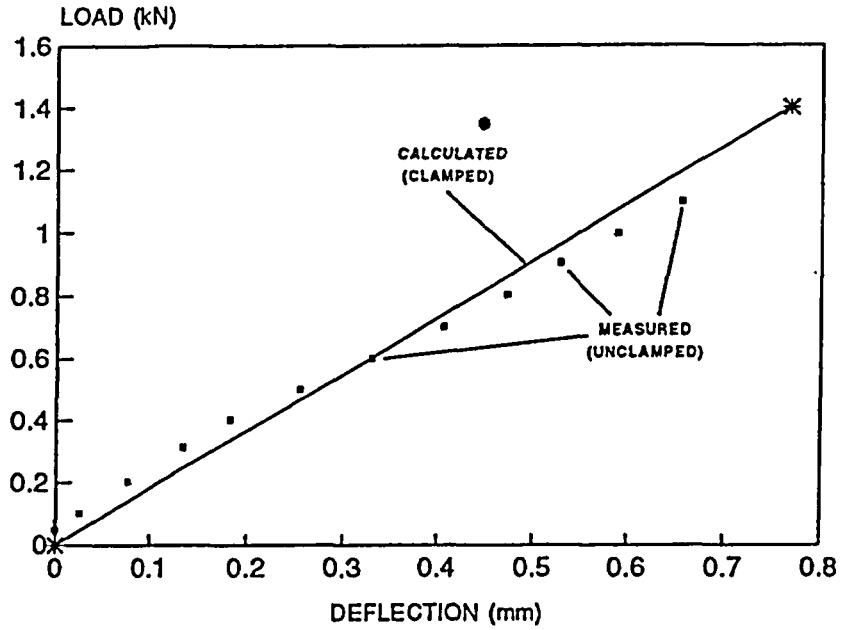

a) Single Fuel Element Plus Pieces of Endplate; Outer Ring

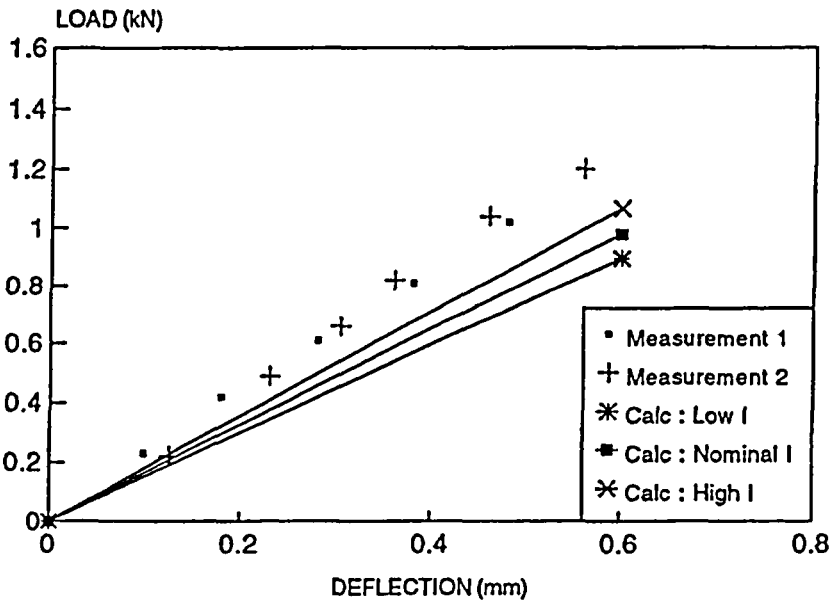

b) Single Fuel Element Plus Pieces of Clamped Endplate; Intermediate Ring
(I = Moment of Inertia)

FIGURE 7: FUEL ELEMENT STIFFNESS WITH PIECES OF ENDPLATES

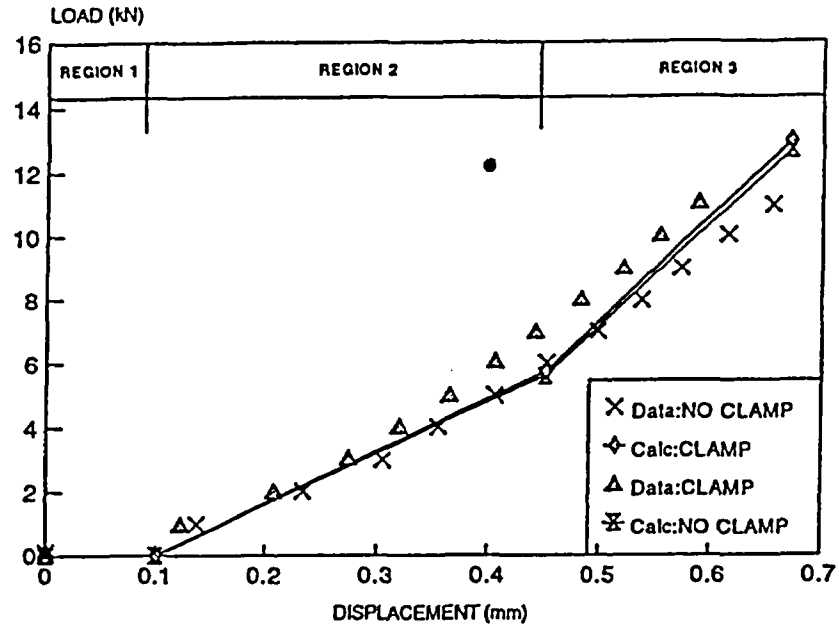

a) Outer Ring Loading: Zircatec Bundle
(Data = Measured; Calc = Calculated)

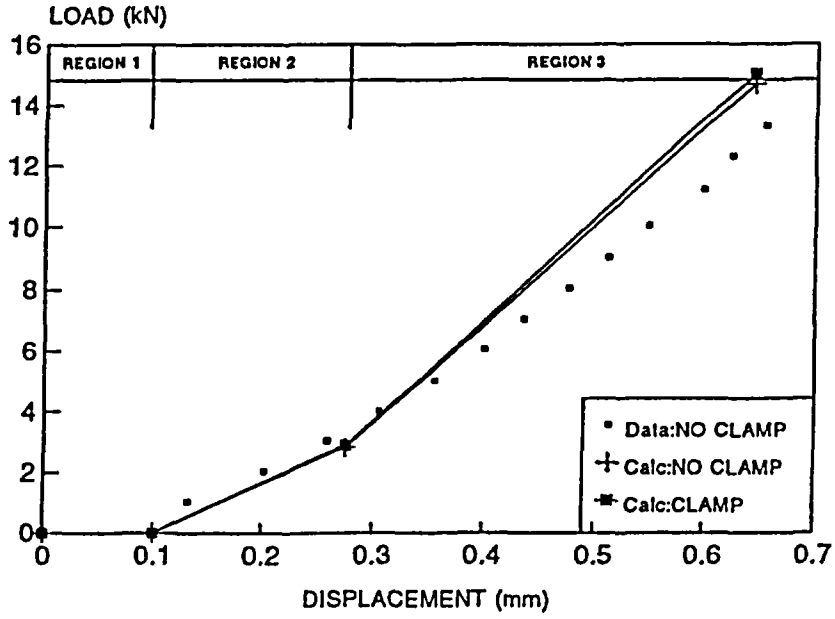

b) Outer Ring Loading: GEC Bundle
(Data = Measured; Calc = Calculated)

FIGURE 8: MEASURED vs. CALCULATED OUTER RING BUNDLE STIFFNESS

EXPERIMENT U118 : BEAM PREDICTIONS vs. EXPERIMENT
(ON POWER FREQUENCY CALCULATIONS vs. DATA)
STARTUP / SHUTDOWN CYCLE # 1

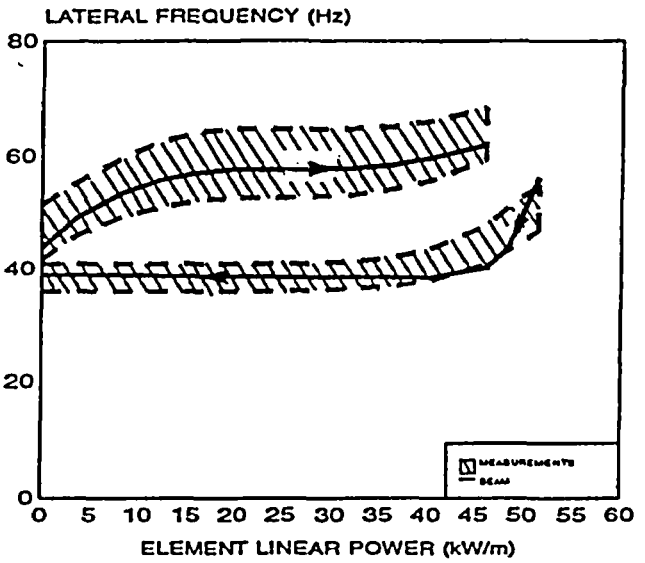

EXPERIMENT U118: BEAM PREDICTIONS vs. EXPERIMENT
(ON POWER FREQUENCY CALCULATIONS vs. DATA)
STARTUP / SHUTDOWN # 2

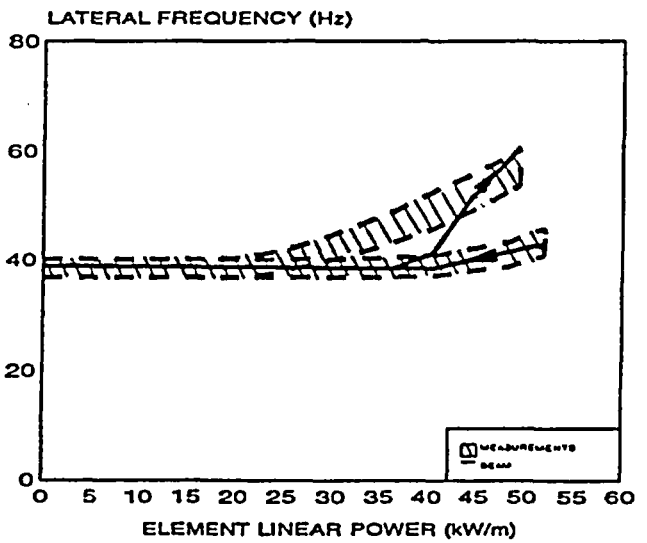

FIGURE 9: U-118 EXPERIMENT vs. MEASURED LATERAL FREQUENCY

POSITION 4
OUTER ELEMENT POWER

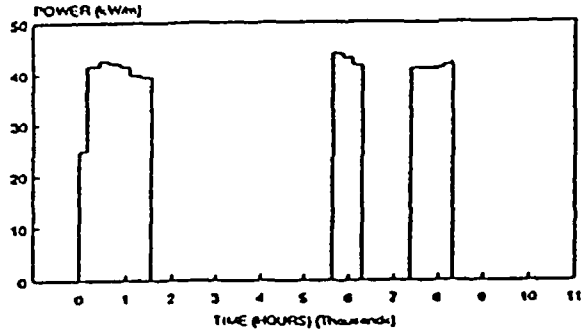

CU: Cold Unpressurized

HP: Hot Pressurized

POSITION 4
PELLET/SHEATH INTERFACE PRESSURE

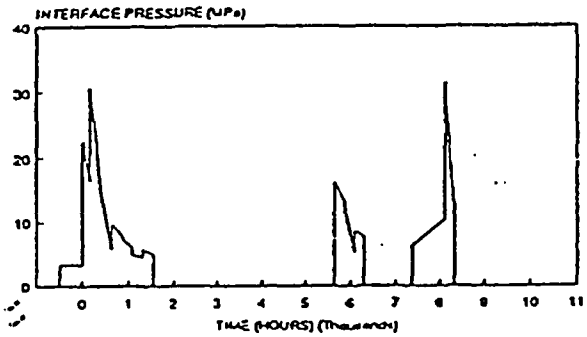

POSITION 4
TOTAL UNCONSUMMED AXIAL GAP

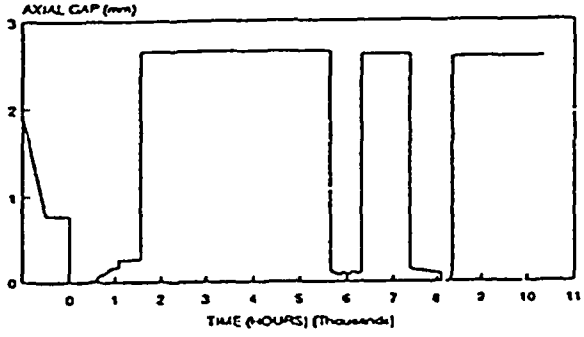

POSITION 4
OUTER ELEMENT AXIAL STIFFNESS

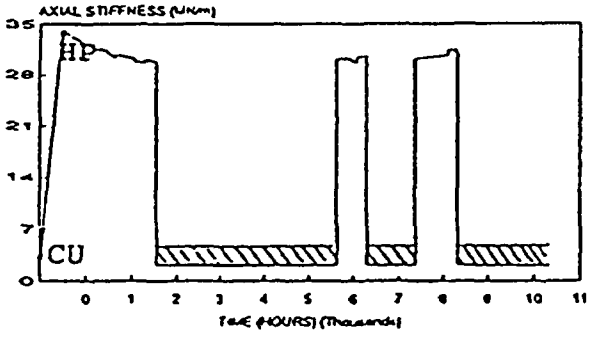

POSITION 4
OUTER ELEMENT FLEXURAL RIGIDITY

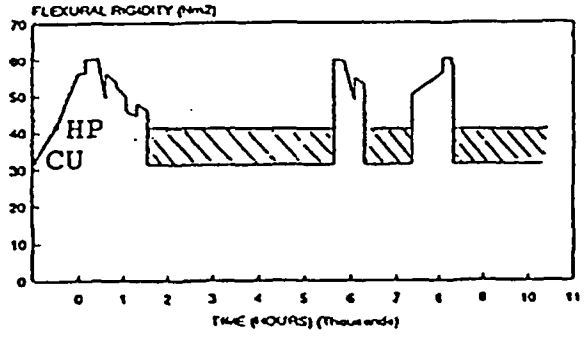

FIGURE 10: OUTER ELEMENT AXIAL STIFFNESS AND FLEXURAL RIGIDITY

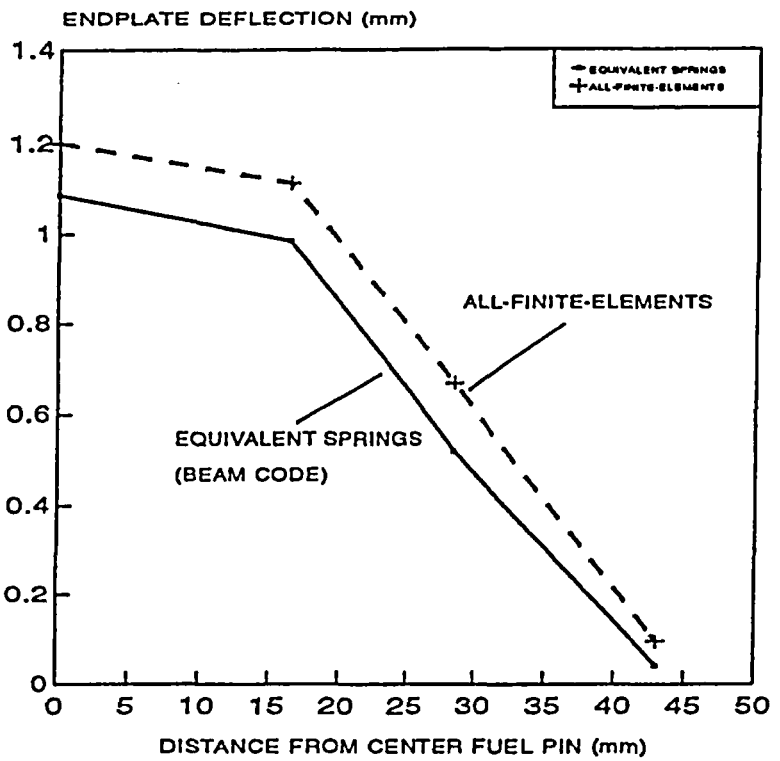

FIGURE 11: EQUIVALENT SPRINGS vs. BEAM FINITE ELEMENTS TO MODEL THE FUEL ELEMENT TO ENDPLATE RESTRAINTS